Eur. Phys. J. D **45**, 295–299 (2007)
DOI: 10.1140/epjd/e2007-00252-0

THE EUROPEAN PHYSICAL JOURNAL D

Direct observation of the non-supported metal nanoparticle electron density of states by X-ray photoelectron spectroscopy

M. Tchaplyguine[1,a], S. Peredkov[2], A. Rosso[1,3], J. Schulz[1,4], G. Öhrwall[3], M. Lundwall[3], T. Rander[3], A. Lindblad[3], H. Bergersen[3], W. Pokapanich[3], S. Svensson[3], S.L. Sorensen[2], N. Mårtensson[1,3], and O. Björneholm[3]

[1] Max-Lab, Lund University, Box 118, 22100 Lund, Sweden
[2] Department of Synchrotron Radiation Research, Box 118, 22100 Lund University, Lund, Sweden
[3] Department of Physics, Uppsala University, Box 530, 75121 Uppsala, Sweden
[4] Department of Physical Sciences, University of Oulu, P.O. Box 3000, 90014 Oulu, Finland

Received 7 March 2007 / Received in final form 14 May 2007
Published online 10 August 2007 –

Abstract. Synchrotron-based X-ray photoelectron spectroscopy on copper and silver cluster beams created by a magnetron-based gas-aggregation source has allowed mapping the electron density of states (DOS) of *free* metallic nanoparticles. The cluster DOS profiles obtained in the experiments strongly resemble the infinite solid DOS shapes, but the extracted cluster work-functions are lower than those for the bulk metal. The latter observation is explained by the initial negative charge on most of the clusters, created by the source.

PACS. 73.22.-f Electronic structure of nanoscale materials: clusters, nanoparticles, nanotubes, and nanocrystals – 79.60.-i Photoemission and photoelectron spectra

Detailed information on the valence band electronic energy structure is of primary importance for understanding nanoparticle-specific properties. When the number of the constituent atoms/molecules becomes countable these properties may differ from those of the macroscopic sample of the same material. It is known, for example, that below a certain number of atoms in a metal cluster the metallic energy structure in the valence region is replaced by a semiconductor-like band structure with a gap between occupied and unoccupied states [1,2]. Such a change leads to the disappearance of metallic conductivity and to the situation when every charge on the sample matters. A direct way to monitor the changes in the valence electron density of states (DOS) is to record a photoelectron spectrum with a sufficiently high photon energy.

The first photoelectron spectroscopy DOS measurements for *supported* metal nanoparticles date back to the end of the 1970s [3,4], where UV lamps and synchrotron radiation were used for their ionization [5]. It was demonstrated that the electronic structure was strongly affected by the interaction with the substrate. First, the nanoparticle structure adjusts to the lattice of the substrate. It causes a distortion in the geometric structure and in the energy-band pattern [6,7]. Second, when the substrate is conducting, an image-charge potential appearing at its surface obscures the changes in such an important measure as the work-function of the nanoparticles [8,9]. In the case of a dielectric substrate the induced polarization and charge accumulation in the sample and the substrate make the situation even worse for the DOS measurements. All these inherent obstacles cause significant difficulties for the photoelectron studies of *supported* metal nanoparticles.

Approximately at the same time as the energy structure of metal *clusters* was first investigated by means of the VUV photoelectron spectroscopy [4–6] the pioneering attempts to approach the same subject, but from the opposite scale-limit — of a few bonded atoms, were performed. Valence levels of *small, free* metal clusters were probed by simple ionization methods [10]. The first experiments were done on the low-melting point metals, for which sufficient cluster concentration could be reached. Photoelectron spectroscopy (PES) on dilute metal cluster beams was not possible in these early years. Somewhat later the introduction of laser vaporization and photoionization mass-spectroscopy methods did allow addressing the electronic structure of clusters of the higher-melting-point-metals, like, for example, copper [11] and silver [12]. However, for quite a long time the development in the *free* metal cluster ionization studies was limited by the achievable cluster sizes. By the end of 90s the largest free metal (copper) cluster for which a photoelectron spectrum was published contained around 400 atoms [13]. And only with the advent of magnetron-based gas aggregation cluster sources [14], which did not really happen until the very first years of the new Millennium, has it become possible

[a] e-mail: maxim@maxlab.lu.se

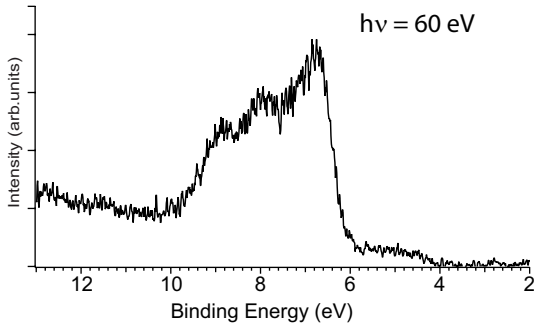

Fig. 1. PES spectrum of nanoscale non-supported copper clusters showing the 3*d* and 4*s* bands (recorded at 60 eV photon energy).

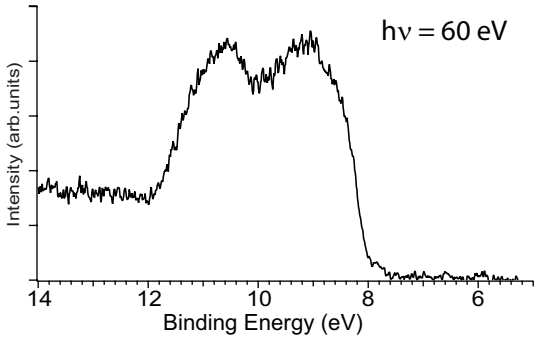

Fig. 2. PES spectrum of nanoscale non-supported silver clusters showing the 4*d* band (recorded at 60 eV photon energy).

to produce and study by PES *free* metal clusters containing up to a hundred thousand atoms [15–19]. The dimensions of the clusters created by such a source can be varied from a few atoms per cluster up to a hundred thousand. The achievable density of the cluster beams has become sufficient to perform *mass-selected* experiments on clusters containing tens of thousands atoms [15]. Measurement of the valence band density of states in principle became possible. However the most-spread modern ionization sources — lasers — used by the majority of the free-cluster community are not able to deliver one-photon energy high enough to probe the whole valence band. Moreover, from the studies of bulk metals it is known that even He VUV-lamp radiation (≈21 eV) doesn't allow mapping the density of states properly. As it has been in the case of *supported* clusters, an optimal ionization source for the studies of *free* nanoparticle DOS is synchrotron radiation.

The present paper reports on the DOS measurements for *free* nanoparticles by means of synchrotron-based X-ray photoelectron spectroscopy. The experimental DOS curves obtained for copper and silver clusters at typical conditions of the magnetron-based free-cluster source operation are presented and briefly discussed at the beginning of the paper. Then follows a detailed description of the apparatus and of the experiment, and more results are given. The discussion following after this is based on comparison of the derived cluster work-functions with the *bulk* metal values, what allows to estimate cluster dimensions. Finally photon energy dependence of the Cu cluster spectrum is presented and compared to that of the polycrystalline bulk DOS.

In Figures 1 and 2 photoelectron spectra of free copper and silver clusters recorded in this work are presented. The relatively high photon energy in use — 60 eV — allows treating the final state in the photoionization process as a free electron continuum, thus avoiding the influence of the conduction band structure on the spectrum, and providing a "clean" mapping of the density of states [20]. A striking resemblance to the polycrystalline bulk copper and silver photoelectron spectra recorded at the same photon energy [20,21] serves as a witness of the well-formed solid-like energy *band* structure in the clusters.

For copper clusters the lower energy part of the 4*s*-band and the 3*d*-band have been recorded (Fig. 1). The main spectral feature — the 3*d* band — has its onset at 6.0 eV binding energy and is about 3.0 eV wide. It has three maxima separated by ≈1 eV, which are also characteristic for a polycrystalline bulk sample spectrum recorded in the angle-integrated mode. One should mention here that clusters need not be polycrystalline but instead can be single crystals. These cluster crystals are however randomly oriented in space when they are irradiated. Thus the structure specific responses are smeared out, and the spectra are noticeably different from those of bulk single crystals [21].

The presence of the 4*s* band lower energy part (Fig. 1), setting on at ≈4.0 eV, allows determining the work-function of the free copper clusters directly — as the lowest energy necessary to remove an electron from the sample into vacuum (i.e. the lowest binding energy of the 4*s* electrons for copper). If one takes the energy at half maximum of the 4*s* band edge then the value for the cluster work-function is ≈4.2 eV.

The spectrum for silver clusters in Figure 2 contains one main feature with two maxima separated by ≈1.4 eV in the band structure — due to the 4*d* electrons. This separation and the 3 eV width of the 4*d* band is the same as in the case of polycrystalline bulk silver. In the solid there is also the 5*s* band at lower binding energies. The signal-to-noise ratio in the present work is such that this feature has not been unambiguously recorded for clusters. (Its intensity in polycrystalline silver probed by angle-integrated-emission PES is also very weak relative to the 4*d* band [20,21].) A direct determination of the silver cluster work-function cannot be made from the spectrum. However the 4*d* binding energy is easily determined: the 4*d* intensity sets on at 7.8 eV and reaches half maximum at 8.2 eV. No narrowing of the band relative to the bulk solid is observed, which was the case for the *supported* clusters on an amorphous graphite substrate [1]. Since the 4*d* band shape is so similar in clusters and in polycrystalline bulk, an assumption on the similarity of the 5*s* bands seems reasonable. In the bulk silver the latter stretches about 4.0 eV below the 4*d*, putting the work-function of silver clusters at ≈4.0 eV. It is worth noting here that conventional single-photon laser ionization could

hardly reach even the foot of the 4*d* band for the clusters under investigation. The highest photon energy achieved in a one-photon process by a laser, namely by a F_2 excimer laser, is 7.9 eV.

As outlined in the beginning, before proceeding with further discussion of the silver and copper cluster photoelectron spectra the details of the experiment will be described.

The magnetron-based gas-aggregation cluster source used in the present study has been described in details in reference [22]. A 2" *US Inc.* magnetron head mounted on a shaft inside a liquid nitrogen cooled cryostat vaporizes metal into the cooled inert gas filling the cryostat. While in the previous work [22] the photoelectron spectroscopy investigation of free metal *atoms* produced by this source was carried out, in the present case the setup has been optimized for the *cluster* production: a narrower and longer Laval-shape exit nozzle was mounted at the tip of the cryostat. The skimmer and the differential pumping arrangement has been removed to allow coming closer to the ionizing radiation, and to simplify the alignment. Only argon gas was used — without any helium admixture — as the magnetron-plasma forming medium, as well as the heat exchanger and the carrier gas. According to the reports on mass-spectroscopy of the gas-aggregation-source-created clusters, pure argon facilitates formation of considerably larger clusters than a mixture of Ar and He [23]. In the present case pure argon has also been used for maintaining a more stable low temperature of the cryostat — in comparison with the experiments where a mixture has been tried. The cryostat was cooled by a continuous flow of pressurized liquid nitrogen. The nozzle temperature was typically at 110–120 K, while the mounting flange of the cryostat was 10–20 degrees warmer. Typical magnetron powers were 250–300 Watts with $\leqslant$1 A plasma current. The distance between the metal target and the cryostat nozzle — "the growth zone" [14–19] was set to be about 12 cm. The input gas pressure was $\approx$2 mbar. As discussed in various papers on the magnetron-based gas aggregation sources such conditions create clusters with up to 10^5 atoms per unit [17].

Photoelectron spectra were recorded using the soft X-ray beamline I411 at the Swedish national synchrotron radiation facility MAX-Lab, and an electrostatic electron energy analyzer (Scienta R4000). The overall energy resolution in the experiments determined by the bandwidth of the radiation and the analyzer instrumental contribution was close to 150 meV. The energy calibration of the spectra was performed using Ar $3p_{3/2}$ line (15.76 eV) appearing in the spectra due to the presence of atomic argon in the ionization volume. The background due to the argon lines is subtracted in the presented spectra.

The cluster source was mounted perpendicular to the synchrotron radiation propagation direction and to the acceptance axis of the analyzer. The latter was fixed vertically — perpendicular to the horizontal polarization plane of the radiation. It is necessary to emphasize that such a geometry is likely to enhance the bulk relative to the surface signal in clusters — due to the elastic scattering of the *d* bulk electrons on their way out of the clusters [24]. In free atoms the 4*d* electrons are ejected mostly along the electric vector direction. In clusters this strong anisotropy in the initial ejection direction is smeared out by the multiple scattering events in the *bulk*, but is preserved to a great extent for the electrons emitted by the *surface*.

The issue of the initial charge possessed by the magnetron-source created clusters deserves a separate discussion. It has been demonstrated that DC-magnetron-based sources produce neutral clusters, as well as cluster ions which may be negative [15,16] or positive [17,18].

It has been theoretically shown that for a *large conducting* metal cluster the initial charge Z (0, +1, or –1) changes the cluster ionization energy $W_{cluster}$ insignificantly [25–27]. Classical and quantum mechanics approaches give similar results for the larger size clusters [25]. In the classical case the ionization potential of a cluster, approximated by a metal sphere, differs from the planar bulk value W_{bulk} due to two reasons. First, due to a different image force potential in the vicinity of a plane surface and of a spherical one. This difference becomes less and less significant with the size since the curvature of the cluster sphere gradually decreases. Second, due to the electrostatic interaction between the charged (in a general case) metallic sphere of a radius R and the ejected electron. The resulting formula (in CGSE units) describes the decrease of the deviation from the solid value with the cluster dimension in the following way [25]:

$$W_{cluster} = W_{bulk} + (Z + 1/2)\frac{e^2}{R}. \qquad (1)$$

A zero or positive initial charge ($Z = 0$, +1) leads to an *increase* in the ionization potential relative to the bulk metal. Converse to this a negative initial charge $Z = -1$ makes the cluster ionization potential *lower* than of the infinite solid. In simple terms the difference for various initial charge states arises due to the presence of the Coulomb interaction between the ejected electron and the metallic sphere in the first two cases, and its absence in the latter. Using electron-Volts as the ionization potential units, Angstroms as the units for the radius R, expression (1) is written as follows:

$$W_{cluster} = W_{bulk} + (Z + 1/2)\frac{14.4}{R(\text{Å})}(\text{eV}). \qquad (2)$$

An excellent agreement with the size dependence predicted by this formula has been demonstrated in numerous experiments on free metal clusters of a smaller (10^1–10^2 atoms) [28], and larger size (10^3–10^4 atoms) in, for example, references [29,30]. Recently an experimental study of the ionization potential dependence on the metal (aluminium) cluster *charge-states* was performed [15], where a more than satisfactory agreement with the expression (1) was obtained for the clusters of 2000 and 30000 atoms.

The ionization potential obtained in the mentioned above experiments can be seen as the cluster work-function — the electron binding energy at the Fermi level. A small difference between the $W_{cluster}$ and W_{bulk} is the

first-level confirmation of the cluster electronic properties approaching those of the bulk. In the present experiments the work-functions derived for both copper and silver clusters — 4.2 eV and 4.0 eV correspondingly — are smaller than the values known for bulk metals. Indeed, in literature the work-function for solid copper is found within the 4.5 to 4.9 eV interval [13,31–33]. For polycrystalline bulk silver one finds the values from 4.0 eV to 4.3 eV [31,34,35]. It means that most of the clusters should be initially *negatively* charged. Such a conclusion is in agreement with the known high concentration of negatively charged clusters created by the magnetron-based sources. The typical sputtering power (300 W) used in the present work is also several times higher than that reported in other papers [14–19]. The knowledge of the difference between the experimental $W_{cluster}$ values and the bulk work-functions allows estimating the cluster dimensions using formulae (1) and (2). Taking $W_{bulk} = 4.5$ eV for copper one can calculate the upper limit for the cluster size: 0.3 eV difference between $W_{cluster}$ and W_{bulk} gives the cluster diameter of ≈5 nm. A similar estimate is obtained for silver clusters if a more recent [35] $W_{bulk} \approx 4.3$ eV value obtained in the studies of a cold silver foil is used. These dimensions fit well to the results of the mass-spectroscopic measurements on a metal cluster beam created by a DC-magnetron based source in reference [17]. Assuming clusters to be of a spherical shape with the density of the solid, one obtains also a size estimate of several thousand atoms/cluster.

The above assumption for the cluster beam charge-composition has been tested in the present experiments using a simple arrangement — an isolated holder comprising two horizontal deflection plates, a grounded field-terminating cylindrical screen and a grounded gold-mesh front screen have been mounted at the tip of the cryostat. When the voltage was applied to the deflection plates (one grounded) no cluster signal was detected with the electron spectrometer. Such a test speaks convincingly for the dominating concentration of the charged particles in the beam over the neutral ones, supporting the conclusions made from the difference in the bulk and cluster work-functions.

Probably no other bulk metal has been as extensively studied by means of photoelectron spectroscopy as copper. For *copper* clusters there is an additional advantage (relative to silver) important from the spectroscopic point of view. In contrast to the 4*d* silver band where, due to the Ag 4*d* Cooper minimum [20], the ionization cross-section decreases drastically within a 50 eV interval above the maximum (at ≈60 eV), the copper 3*d* cross-section gradually increases by an order of magnitude from 40 to 120 eV and then stays practically constant up to at least 250 eV [20]. This has allowed us to study the 3*d* copper band photon energy dependence in the present case of *free* nanoparticles in a low density cluster beam. Figure 3 presents three copper cluster spectra for different photon energies — 60 eV, 108 eV, and 130 eV — obtained at the same clustering conditions. We have compared our results with the polycrystalline copper spectra published in references [20,21], though the considerably worse resolution

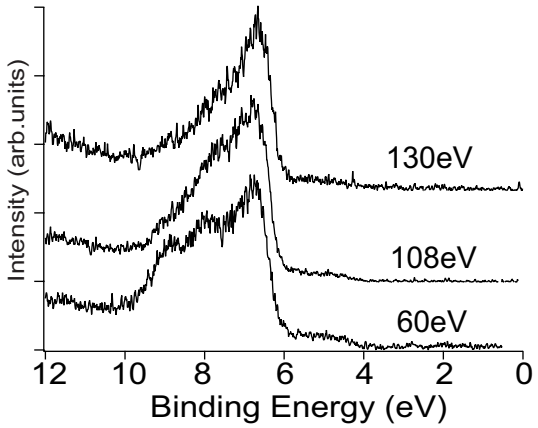

Fig. 3. PES of copper valence bands for three different photon energies: 60 eV, 108 eV, and 130 eV.

in the latter works — 0.35 eV — complicates this comparison. There are perhaps more similarities than differences in the photon energy dependence observed for the clusters and for polycrystalline copper. In both cases the three peaks in the DOS of copper at $h\nu \approx 60$ eV merge into a structureless feature at higher photon energies. In both cases the peak lowest in binding energy (at ≈6.8 eV in Fig. 3) seems to grow in intensity relative to the higher binding energy peaks when the photon energy is increased. In the study of the bulk polycrystalline copper [20] the observed spectral behaviour was explained by "a growing number of the final states available with the photon energy increase, and by a more complete sampling of the valence band arising from an uncertainty in the final state momentum". These reasons for the spectral changes must also apply to the clusters.

One can also underline the differences in electron acquisition in the discussed studies of solid polycrystalline copper and in the present cluster studies. In the former case the angle-integrated collection of electrons from polycrystalline metal was implemented. In the latter case the normal-to-light cluster beam was sampled within a small solid angle perpendicular to the polarization plane of the radiation. As mentioned above the ejected *d*-electrons are initially highly anisotropic. Those from the bulk become much more uniform in their angular distribution after efficient elastic scattering within the cluster [24]. Thus in the present experiment the geometric configuration emphasizes the response of the cluster bulk over the surface. In the angle-integrated case all electrons are collected, and bulk-surface specificity due to the difference in angular distribution is lost. Another peculiarity of the cluster beam experiment is a somewhat different sampling of the bulk and surface layers in spherical nanoscale clusters and in planar infinite solids. Indeed in the clusters of the size in question the surface atoms constitute a significant fraction of the total amount of atoms, while in planar solid samples this fraction is negligible. Thus the bulk electron flux attenuation influences the spectra of the clusters more than those of the solid bulk sample. Indeed, with the kinetic energy decreasing the electron escape depth steeply increases

below 70 eV [20] in copper. For the present case the copper electrons with $E_{kin} \approx 50$ eV ($h\nu = 60$ eV) have about three times larger mean free path — 0.6 nm — than those with 100 eV ($h\nu = 108$ eV), and 120 eV ($h\nu = 130$ eV). It makes the 60 eV measurement the most bulk-sensitive in the series. Taking all these considerations into account one can conclude that the features at about 8 and 9 eV binding energies pronounced in the bulk-sensitive spectrum at $h\nu = 60$ eV could be predominantly due to the electrons from the inner parts of the clusters. This conclusion is in accord with, for example, the early PES studies [36] of the layer-by-layer grown copper adsorbates, where the two characteristic higher binding energy features appeared only with more than two monolayers coverage. Also in somewhat later DOS measurements [37] of copper *two-dimensional* islands grown on crystalline graphite a narrow structureless $3d$ peak was recorded which at higher coverage transformed into the lowest binding energy feature. Similar conclusions concerning the assignment of various peaks in the DOS were made in a theoretical work [38] where the lowest binding energy feature was calculated to be due to the surface-emitted electrons.

Summarizing the results of the present work one can state that the technically challenging synchrotron-based X-ray photoelectron spectroscopy on non-supported nanoscale metal clusters has proven to be feasible. The spectrum analysis has allowed obtaining important parts of the electron densities of states for the clusters under investigation, deriving cluster work-functions, determining the initial negative charge-state of the clusters, and estimating the cluster size in a good agreement with the expectations. A photon energy dependence study of copper cluster spectra suggests that the higher binding energy part of the spectrum originates from atoms in the bulk.

We gratefully acknowledge the financial support of the Knut and Alice Wallenberg Foundation, the Swedish Foundation for Strategic Research (SSF), the Göran Gustafsson Foundation and the Swedish Research Council (VR).

References

1. G.K. Wertheim, Phase Transitions **24-26**, 203 (1990)
2. B.V. Issendorff, O. Cheshnovsky, Annu. Rev. Phys. Chem. **56**, 549 (2005)
3. W.F. Egelhoff Jr, G.G. Tibbetts, Sol. St. Comm. **29**, 5357 (1979)
4. R.C. Baetzold, Surf. Sci. **106**, 243 (1981)
5. G.K. Wertheim, S.B. DiCenzo, D.N.E. Buchanan, Phys. Rev. B **37**, 5384 (1986)
6. G.K. Wertheim, S.B. DiCenzo, S.E. Youngqvist, Phys. Rev. Lett. **51**, 2310 (1983)
7. G.K. Wertheim, Z. Phys. D **12**, 319 (1989)
8. S. Di Nardo, L. Lozzi, M. Passacantando, P. Picozzi, S. Santucci, M. De Crescenzi, Surf. Sci. **307-309**, 922 (1994)
9. S.L. Qiu, X. Pan, M. Strongin, P.H. Citrin, Phys. Rev. B **36**, 1292 (1987)
10. A. Herrmann, E. Schumacher, L. Wöste, J. Chem. Phys. **68**, 2327 (1978)
11. M.B. Knickelbein, Chem. Phys. Lett. **192**, 129 (1992)
12. G. Alameddin, J. Hunter, D. Cameron, M.M. Kappes, Chem. Phys. Lett. **192**, 122 (1992)
13. O. Cheshnovsky, K.J. Taylor, J. Conceicao, R.E. Smalley, Phys. Rev. Lett. **64**, 1785 (1990)
14. H. Haberland, M. Mall, M. Moseler, Y. Qiang, Th. Reiners, Y. Thurner, J. Vac. Sci. Technol. A **12**, 2925 (1994)
15. M. Astruc Hoffmann, G. Wrigge, B.v. Issendorff, Phys. Rev. B **66**, 041404(R) (2002)
16. H. Häkkinen, M. Moseler, O. Kostko, N. Morgner, M. Astruc Hoffmann, B.v. Issendorff, Phys. Rev. Lett. **93**, 093401 (2004)
17. R. Morel, A. Brenac, P. Bayle-Guillemaud, C. Portemont, F. La Rizza, Eur. Phys. J. D **24**, 287 (2003)
18. H. Yasumatsu, T. Hayakawa, S. Koizumi, T. Kondow, J. Chem. Phys. **123**, 124709 (2005)
19. S. Pratontep, S.J. Carroll, C. Xirouchaki, M. Streun, R.E. Palmer, Rev. Sci. Instr. **76**, 045103 (2005)
20. D.A. Shirley, J. Stöhr, P.S. Wehner, R.S. Williams, G. Apai, Phys. Scripta **16**, 398 (1977)
21. J. Stöhr, G. Apai, P.S. Wehner, F.R. McFeely, M.S. Williams, D.A. Shirley. Phys. Rev. B **14**, 5144 (1976)
22. M. Tchaplyguine, S. Peredkov, H. Svensson, J. Schulz, G. Öhrwall, M. Lundwall, T. Rander, A. Lindblad, H. Bergersen, S. Svensson, M. Gisselbrecht, S.L. Sorensen, L. Gridneva, N. Mårtensson, O. Björneholm, Rev. Sci. Instr. **77**, 033106 (2006)
23. U. Zimmermann, N. Malinowski, U. Niiher, S. Frank, T.P. Martin, Z. Phys. D **31**, 85 (1994)
24. G. Öhrwall, M. Tchaplyguine, M. Gisselbrecht, M. Lundvall, R. Feifel, A. Lindgren, N. Mårtensson, S. Svensson, O. Björneholm, J. Phys. B: At. Mol. Opt. Phys. **36**, 3937 (2003)
25. G. Makov, A. Nitzan, L.E. Brus, J. Chem. Phys. **88**, 5076 (1988)
26. D.M. Wood, Phys. Rev. Lett. **46**, 749 (1981)
27. M. Seidl, J.P. Perdew, M. Brajczewska, C. Fiolhais, J. Chem. Phys. **108**, 8182 (1998)
28. K. Rademann, B. Kaiser, U. Even, F. Hensel, Phys. Rev. Lett. **59**, 2319 (1987); and references therein
29. K. Wong, V. Kasperovich, G. Tikhonov, V.V. Kresin, Appl. Phys. B: Lasers Opt. **73**, 407 (2001)
30. A. Schmidt-Ott, P. Schurtenberger, H.C. Siegmann, Phys. Rev. Lett. **45**, 1284 (1980)
31. D.E. Eastman, Phys. Rev. B **2**, 1 (1970)
32. C. Nordling, J. Österman, *Physics Handbook* (Chartwell-Bratt, 1980).
33. P.A. Tipler, R.A. Llewellyn, *Modern Physics*, 3rd edn. (W.H. Freeman, 1999)
34. A. Barrie, N.E. Christensen. Phys. Rev. B **14**, 2442 (1976)
35. C.W. Kim, J.C. Villagran, U. Even, J.C. Thompson, J. Chem. Phys. **94**, 3974 (1991)
36. D.E. Eastman, W.D. Grobman, Phys. Rev. Lett. **30**, 177 (1973)
37. W.L. Egelhoff Jt, G.G. Tibbetts, Sol. St. Comm. **29**, 53 (1978)
38. J.A. Appelbaum, D.R. Hamann, Sol. St. Comm. **27**, 881 (1978)